1. Theories of GRBs

1.1. **Introduction.** Gamma-ray bursts are relativistic fireballs originating from the birth of black holes at great cosmological distances. A large fraction of long bursts are detected with a mean redshift $z \sim$ DERMER's book pg 9 says 1. It is appropriate to provide a quick review on topics from cosmology and special relativity that will be important in this dissertation.

1.2. **Cosmology.** The cosmological principle is the notion that our universe is homogeneous and isotropic and therefore has no specific locations or directions marking the origin or future destination. The universe appears to have the exact same conditions to all observers at all locations at the same time. This notion of isotropy and homogeneity is a direct result of the initial hot dense state of our universe in equilibrium within a singularity. Observations of the cosmic microwave background radiation (CMB) are largely isotropic in intensity in all directions as well as the large-scale structure ($\gtrsim$ 100 Mpc) of galactic filaments and voids. However, at the scale of galaxy groups and clusters, the universe exhibits pronounced anisotropy but is irrelevant for the studies of gamma-ray bursts at great cosmological distances. Therefore, all calculations in this section are based on a homogeneous and isotropic universe with flat spatial geometry and observational evidence of these basis will be addressed at a later time.

We begin with the Robertson-Walker metric to determine spacetime intervals and the effects of cosmological expansion on times, distances, energies and luminosities. This metric only holds on the large scale as it represents a homogeneous and isotropic universe. At smaller scales, about the size of galactic clusters and smaller, the universe is profoundly anisotropic. All particles follow a geodesic trajectory through four-dimensional spacetime given by the Robertson-Walker metric,

$$(1)\quad ds^2 = -c^2dt^2+dx^2+dy^2+dz^2 = -c^2dt^2+d\vec{r}^2 = -c^2dt^2+dr^2+r^2d\theta^2+r^2sin^2\theta d\phi^2$$

shown here in both cartesian and polar coordinates. This geodesic is invariant, the same in all inertial frames, and useful for deriving the proper time for particles associated with real events. The variational principle for the motion of free particles states that the geodesic path of a free particle between two timelike ($ds < 0$) events extremizes the proper time between them (Hartle book pg 89). Therefore, if you have two events in spacetime, A and B, a free particle will travel between the two along a geodesic ds with a stationary proper time (τ). Proper time of a geodesic is defined as the distance traveled along it given by $\Delta\tau^2 = -ds^2/c^2$ and has units of time. Photons follow a null geodesic where $ds = 0$, making a light cone in Minkowski space. Timelike events such as A and B mentioned above are confined within this light cone, are causally connected and therefore are considered to be real events.

Events outside the light cone, where $ds > 0$, are said to be spacelike and can not be causally connected. These events are of no concern to us.

The metric can be written to account for cosmological expansion and geometric curvature as

$$ds^2 = -c^2dt^2 + \mathcal{A}^2(t)\left[\frac{dr^2}{1-kr^2} + r^2\left(d\theta^2 + sin^2\theta d\phi^2\right)\right] \tag{2}$$

where $\mathcal{A}(t)$ is the dimensionless expansion scale factor, (r, θ, ϕ) are the comoving coordinates at some point in space and k is the curvature index. The scale factor describes how distances in the universe expand with time and we normalize it to the present time so that $\mathcal{A}(t_0) = 1$. The comoving coordinates (r, θ, ϕ) must remain at rest within the Hubble flow for the universe to be perfectly homogeneous and isotropic, and therefore do not change with time. The curvature index can take on a value in the range from $+1$ for a closed spherical geometry to -1 for an open hyperbolic geometry. The case where $k = 0$ provides a flat geometry with absence of curvature at a large scale. TALK ABOUT HOW OBSERVATIONS SUPPORT A FLAT UNIVERSE.

We now use the metric to determine the effects cosmological expansion have on light as it propagates great cosmological distances. Consider a photon is emitted at some time t_e in the past and travels radially toward an observer so that $d\theta = d\phi = 0$, where $ds = 0$ for a photon. In a flat universe where $k = 0$, the metric becomes $0 = -c^2dt^2 + \mathcal{A}^2(t)dr^2$. If we imagine two successive wave crests of light are emitted, the first at t_e and the second at $t_e + \Delta t_e$ then they must be observed at times t_0 and $t_0 + \Delta t_0$. The comoving coordinate r remains constant with time $\Delta r = 0$ and can be written as,

$$r = c\int_{t_e}^{t_0}\frac{dt}{\mathcal{A}(t)} = c\int_{t_e+\Delta t_e}^{t_0+\Delta t_0}\frac{dt}{\mathcal{A}(t)}. \tag{3}$$

With some assumptions and re-arranging of integration limits, we arrive at the expression

$$\frac{\Delta t_0}{\mathcal{A}(t_0)} = \frac{\Delta t_e}{\mathcal{A}(t_e)} \quad \text{or} \quad \Delta t_0 = \frac{\Delta t_e}{\mathcal{A}(t_e)}, \tag{4}$$

since $\mathcal{A}(t_0) = 1$. Assumptions: (1) the period between the emitted (Δt_e) and observed (Δt_0) wave crests are small enough so that $\mathcal{A}(t)$ is a constant and (2) peculiar velocities of the emitters are negligible. From measuring the period of light Δt, one can arrive at the wavelength, frequency and energy from the following relationships,

$$\lambda = c\Delta t, \quad \nu = \frac{1}{\Delta t} = \frac{c}{\lambda}, \quad \text{and} \quad E = h\nu \tag{5}$$

where c is the speed of light in a vacuum and h is Planck's constant.

The measured shift in a galaxy's absorption and emission lines from the lab frame to the observed frame is proportional to its distance, give by the formula

$$z \equiv \frac{\lambda_0 - \lambda_e}{\lambda_e} = \frac{\lambda_0}{\lambda_e} - 1 \quad \text{or} \quad z + 1 = \frac{\lambda_0}{\lambda_e}. \tag{6}$$

Equation 6 is valid at small redshifts $z \ll 1$ and can be treated as the nonrelativistic Doppler shift where $z = v/c$ and Hubble's law becomes $v = H_0 d_p$ or $z = H_0 d_p/c$, where v is the radial velocity of the galaxy, H_0 is Hubble's constant and d_p is the proper distance. From equations 4, 5 and 6 we arrive at an expression between the expansion parameters and reshift,

$$\frac{\lambda_0}{\lambda_e} = \frac{\mathcal{A}(t_0)}{\mathcal{A}(t_e)} = \frac{1}{\mathcal{A}(t_e)} = 1 + z. \tag{7}$$

Equation 4 describes the cosmological time dilation; the observed delay between wave crests will be longer than emitted by a factor of $1 + z$. Equation 7 describes the cosmological redshift; the wavelength observed will be longer than emitted by a factor of $1 + z$.

The proper distance is found by integrating over the radial comoving coordinate r,

$$d_P(t) = \mathcal{A}(t) \int_0^r dr = \mathcal{A}(t) r = (1 + z) r. \tag{8}$$

The comoving distance d_c between two objects in space remains constant with time if the two are moving with the Hubble flow and can be found by multiplying the proper motion at the present epoch by a factor of $1 + z$,

$$d_c = r = d_p(t_0)(1 + z). \tag{9}$$

Because the comoving coordinate r is constant, integrating over the proper distance with respect to the cosmological time coordinate gives the change in proper distance between us and the emitter over time,

$$\dot{d_P}(t) = \dot{\mathcal{A}}(t) r = \frac{\dot{\mathcal{A}}(t)}{\mathcal{A}(t)} d_P, \tag{10}$$

$$\dot{d_P}(t) = c\Delta t = \dot{\mathcal{A}}(t) r = \frac{\dot{\mathcal{A}}(t)}{\mathcal{A}(t)} d_P, \tag{11}$$

or what is also known as, Hubble's Law. Hubble's constant for anytime in the past can be written as $H(t) = \dot{\mathcal{A}}(t)/\mathcal{A}(t)$, where $H_0 = 67.8 \pm 0.9$ is the value at the present day, as measured by the *Planck* telescope [CITE 2015 paper Planck 2015 results. I. Overview of products and scientific results]. Hubble's constant .

The comoving distance along the line of sight is the radial comoving coordinate, r, and from equation 8 we find

$$d_c = d_p(t_0)(1+z) = d_H \int_0^z \frac{dz'}{\epsilon(z')} \tag{12}$$

where $d_H = c/H_0$ is the Hubble distance and the function

$$\epsilon(z) \equiv \sqrt{(1+z)^3\ \Omega_M + (1+z)^2\ \Omega_k + \Omega_\Lambda}\ , \tag{13}$$

which is proportional to the time derivative of the logarithm of the scale factor (i.e. $\dot{\mathcal{A}(t)}/\mathcal{A}(t) = H(t)$), with z redshift and Ω_M, Ω_k and Ω_Λ are the mass, curvature and energy density parameters, respectively. For a flat universe, $\Omega_k = 0$. Because distance in space can not realistically be measured with a ruler, the luminosity distance relationship is used,

$$d_L = d_T(1+z) = \frac{c}{H_0}(1+z) \int_0^z \frac{dz'}{\sqrt{(1+z)^3\ \Omega_M + \Omega_\Lambda}} \tag{14}$$

where d_T is the transverse comoving distance and is equal to the line of sight comoving distance in a flat universe.

The luminosity distance can also be written as,

$$d_L \equiv \sqrt{\frac{L}{4\pi\phi}} \tag{15}$$

where ϕ is the bolometric flux and $L = dE/dt$ is the bolometric luminosity. The bolometric flux can not be measured because the bandpass from which photons were emitted becomes redshifted and must be corrected to the observed bandpass by a factor called the k-correction. For GRBs we use S to represent the fluence of a burst found from the equation

$$S_{[e_1,e_2]} = \int_{e_1}^{e_2} E\ S_0\ \phi(E) dE \int_{t_1}^{t_2} dt \tag{16}$$

where e_1 and e_2 are the observed energies, $t_2 - t_1$ is the observed burst duration, S_0 is a normalization (with units of photons per unit area per unit energy) and $\phi(E)$ is the time-integrated flux as a result of the spectral shape with energy. Both $\phi(E)$ and S_0 are found through spectral modeling of the prompt emission.

We rewrite the equation to give the relationship between the bolometric (isotropic equivalent) energy in the burst frame and the differential fluence of the observed frame as

$$E_{iso} = E_{[E_1,E_2]} = \frac{4\pi d_L^2}{1+z} S_{[e_1,e_2]}\ k_{cor}. \tag{17}$$

We choose to measure all GRBs at the same bandpass in the burst's rest frame of $E_1 = 10$ keV to $E_2 = 10$ MeV and apply the k-correction,

$$k_{cor} = \frac{S_{[E_1/(1+z),E_2/(1+z)]}}{S_0}\frac{S_0}{S_{[e_1,e_2]}} = \frac{S_{[E_1/(1+z),E_2/(1+z)]}}{S_{[e_1,e_2]}} \tag{18}$$

to the observed fluence, $S_{[e_1,e_2]}$. You can see from the equation above that $e_1 = E_1/(1+z)$ and $e_2 = E_2/(1+z)$ when $k_{cor} = 1$, therefore we shift the redshifted observed bandpass until it matches the fixed comoving bandpass (the burst's rest frame). The factor of $(1+z)$ in equation 17 relates the observer time to the burst frame time, $\Delta t_0 = \Delta t_e(1+z)$, associated with the time integration hidden within the fluence equation 16; commonly pulled out front since it is a constant.

For GRBs, the isotropic equivalent energy then becomes,

$$E_{iso} = \frac{4\pi d_L^2}{1+z}\int_{\frac{E_1}{(1+z)}}^{\frac{E_2}{(1+z)}} E S_0 \phi(E) dE \int_{t_1}^{t_2} dt. \tag{19}$$

We will leave the discussion of the usefulness of this energy and the spectral modeling of $\phi(E)$ and S_0 to a future section.

[?] [?] [?] [?] [?]

1.3. **Special Relativity and Reference Frames.** We must discuss the special relativistic effects when matter particles are traveling at velocities close to the speed of light and what that looks like between the three frames of reference: (1) the comoving frame, the rest frame of the Hubble flow, (2) the source emitting frame, the rest frame of the GRB jet at any given point, and (3) the observer's frame on Earth, the rest frame of the observer.

The comoving frame is the rest frame of the Hubble flow of the Universe and will be denoted with a *com* subscript (K_{com} frame). The stellar emitting frame moves with some velocity v relative to the comoving frame and will be denoted with a primed symbol (K' frame). A Lorentz transformation needs to be done between the two frames since the stellar frame is moving with a constant velocity, its pecular velocity, relative to the Hubble flow. It is common to adopt the prime symbol for the moving frame and unprimed for the stationary rest frame.

Many texts adopt the comoving frame to be the rest frame of the emitting object under consideration. This is only valid in two cases. The first is when the object is truly at rest relative to the Hubble flow because it has no pecular velocity. The second is when the time separation between two events in all reference frames are small enough that the pecular velocity relative to the Hubble flow is negligible. If the time separation between the two events in both frames ($dt' = t_2' - t_1'$ and $dt = t_2 - t_1$) are on the order of a visible wavelength's period, then Lorentz transformations between the comoving and other two frames can be ignored.

Consider the two events to be the emission of two consecutive photons from a charged particle moving in a relativistic jet. The time between emission in the charged particles rest frame (K') is denoted dt' where there Earth observer receives the two photons separated by a time dt, where $dt \neq dt'$. To determine how these two quantities compare between frames, both relativistic effects of time dilation and time retardation need to be accounted for.

The simplest case is to align the x-axes of the two frames we wish to switch between so that Lorentz transformations can be done to compare quantities between them. Frame K' moves with a relativistic speed ($+\beta = v/c$) relative to K along the aligned x-axes which is also aligned with the Earth observer's line of sight. The Lorentz transformations of coordinates between frames are

$$\begin{aligned} t' &= \Gamma\left(t - \frac{\beta x}{c}\right) \\ x' &= \Gamma\left(x - \beta c t\right) \\ y' &= y \\ z' &= z \end{aligned} \tag{20}$$

where $\beta = v/c$ is the speed of the charged particle as a fraction of the speed of light. The reverse transformations can be found by changing $+\beta$ to $-\beta$ and swapping the symbols on the x and t dimensions. The y and z axes remain unchanged between frames since there is no relative motion along these axes in this simple case. The speed of a relativistic jet is represented by its bulk Lorentz factor Γ given by

$$\Gamma = \frac{1}{\sqrt{1-\beta^2}} \tag{21}$$

where $\beta = v/c$ is the average speed of individual particles within the jet. Particles within the jets of Gamma-ray bursts move at highly relativistic speeds where $\Gamma \gg 1$.

Proper time and proper length are invariant quantities of time and distance as measured in the rest frame of the moving particle, relative to the observer's frame.

Proper time is the time difference between two events as measured by a clock at rest in the frame of the events. A charged particle is at rest at the origin $x' = 0$ of frame K'. An interaction with the charged particle releases two photons from the origin, one at $t_1^{'}$ and a second at $t_2^{'}$. A clock in this frame measures the proper time to be $dt' = t_2^{'} - t_1^{'}$. Frame K' is moving relative to an observer's stationary frame K with some velocity β. The outside observer receives the two photons at times t_1 and t_2. From equation 20, we find the observer's clock to measure $dt = dt'\Gamma$ to be longer than the proper time. The clock of the moving particle, the proper time, runs slower and therefore less time passes compared to the observer's clock. This is called time dilation in relativistically moving frames.

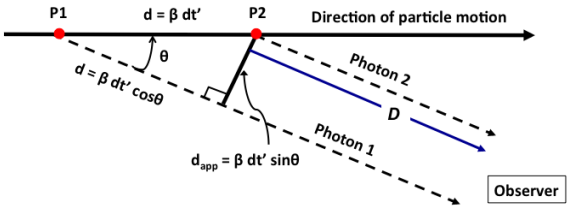

FIGURE 1. A charged particle moves a distance $\beta dt'$ at an angle θ to the observer's line of sight and emits two photons, one at P1 at time $t_1^{'}$ and a second at P2 at time $t_2^{'}$. The observer sees the emitter moving along an apparent path transverse to the line of sight along $\beta dt' \sin\theta$ in time $dt = t_2 - t_1$, the time between reception of the two photons. Photon 2 arrives before photon 1 and the source appears to have a velocity > c. This is called superluminal motion.

Proper length refers to the length an object has while at rest within its own frame of reference. Consider a ruler at rest in K', but it moves with its frame velocity β relative to a stationary observer in the K frame. If both ends are measured simultaneously in K ($dt = t_2 - t_1 = 0$) from equation 20, the observer in the K frame measures a length of $dx = dx'/\Gamma$. An outside observer in a stationary K frame will find the ruler to have a shorter length dx than its true proper length dx'. This is called length contraction.

KIM, keep this. *Observer Length* $= \frac{Proper\ Length}{\Gamma}$ and *Observed Time* $= \Gamma \times$ *Proper Time.*

Time dilation and length contraction arise from switching between the two coordinate frames, but is not the only effect on times and distances. Times and distances become retarded when the motion of the charged particle is not aligned with the observer's line of sight, but it emits photons that are. The charged particle moves at angle θ' relative to the observer's line of sight in K' and θ in K with velocity β and emits two photons at times $t_1^{'}$ and $t_2^{'}$ and positions $P_1^{'}$ and $P_2^{'}$, respectively. See Figure 1. The time of reception between the two photons becomes

$$dt = dt^{'}(1 - \beta\cos\theta) \tag{22}$$

and the distance between the apparent emission sites is

$$dx = \frac{dx^{'}}{(1 - \beta\cos\theta)}. \tag{23}$$

Combining the two effects we get the total delay between photons in the observer frame to be

$$dt = dt^{'}\Gamma(1 - \beta\cos\theta) \tag{24}$$

and distance traveled (or length of an object) in the observer frame to be

$$dx = \frac{dx^{'}}{\Gamma(1 - \beta\cos\theta)}. \tag{25}$$

Applying this to other properties of light, we get

$$\frac{dt_{emit}}{dt_{obs}} \propto \frac{\nu_{obs}}{\nu_{emit}} \propto \frac{\lambda_{emit}}{\lambda_{obs}} = \frac{1}{\Gamma(1 - \beta\cos\theta)} \tag{26}$$

where $\lambda = c/\nu = c\ dt$.

This difference between frames is called the Doppler factor and can be written as

$$\begin{aligned} \mathcal{D} &= \frac{1}{\Gamma\,(1 - \beta cos\theta)} \quad \text{for } \theta \gg 1^{\circ} \\ \mathcal{D} &\longrightarrow \frac{2\Gamma}{1 + \Gamma^2\theta^2} \qquad \text{for } \Gamma \gg 1 \text{ and } \theta \ll 1^{\circ}, \end{aligned} \tag{27}$$

where θ is the angle as observed from Earth. The first part of the Doppler factor is for all viewing angles off the observer's line of sight and the second for the limit when θ approaches the line of sight as a result of $(1 - \beta\cos\theta)^{-1} \rightarrow 2\Gamma^2/(\Gamma\theta + 1/\Gamma\theta)$ for $\Gamma \gg 1$ and $\theta \ll 1^{\circ}$. For the first part, when $\theta = \pi/2$ and $\cos\theta = 0$ we obtain the transverse Doppler effect and the Doppler factor becomes Γ^{-1}. At the critical angle discussed below, $\theta = \Gamma^{-1}$, we get a Doppler factor of Γ. For the second part, when $\theta = 0$, we get a radial Doppler factor of $\sim 2\Gamma$. This can be seen in Figure 2.

From Figure 1 we can see that the source emitting photons appears to move a distance of $dx = \beta dt'\sin\theta$ in time dt. With use of equation 24, we get that the source has an apparent velocity of

$$\beta_{app} = \frac{\beta\sin\theta}{1 - \beta\cos\theta} \text{ for } \theta \gg 1^{\circ} \tag{28}$$

and for $\Gamma \gg 1$, $\beta_{app} > c$ and the source exhibits superluminal motion. The apparent velocity is maximized at the critical angle of Γ^{-1}, giving $\cos(\Gamma^{-1}) \approx \beta$ and the maximum apparent velocity becomes $\beta_{app} = \beta\Gamma$. We obtain velocities $> c$ because the source appears to be moving transverse to our line of sight, along $d = \beta dt\sin\theta$ in figure 1, but is actually moving along $d = \beta dt$, at an angle θ toward us. Therefore, the photons emitted at a later time when the source is closer to us, at $P2$, are received before those emitted earlier and at a greater distance, at $P1$. At the angle

$\theta = \pi/2$ we get an apparent velocity that is equal to the true velocity, β. Again, for the limiting case when $\theta \sim 0$, equation 28 becomes

$$\beta_{app} \longrightarrow \frac{2\Gamma^2}{\Gamma^2\theta^2 + 1} \text{ for } \theta \longrightarrow 0 \tag{29}$$

and the apparent velocity, if the partial were moving radially toward the observer, would be $2\Gamma^2$. Superluminal motion is possible anytime $\Gamma > \sqrt{2}$.

Kim, the primed and unprimed are exactly backward from Hartle's GR book on this.

Now, instead of a charged particle moving at an angle relative to the observers line of sight, a photon is emitted at some angle. The same concept as the particle can be used, but with $v = v' = c$. The angle θ' is the angle between the direction the photon was emitted and the observer's line of sight and θ is that angle as seen from the Earth observer's frame. The relationship between these two angles is given by

$$\cos\theta = \frac{\cos\theta' + \beta}{1 + \beta\cos\theta'}. \tag{30}$$

The light emitted from the forward facing hemisphere ($\theta' < \pi/2$) is beamed into a smaller angle θ, giving a greater intensity to the observed brightness. This effect is called Doppler boosting (or beaming) and occurs along the axis of the relativistic source's motion. For all photons movings directly toward the observer, where $\theta = 0$, the light is blueshifted and all photons moving directly away from the observer, where $\theta = \pi$, the light is redshifted, according to equation 26.

If we account for all cosmological and relativistic effects, the total Doppler shift becomes

$$\mathcal{D}_{total} = \frac{\mathcal{D}_{rel}}{(1+z)} = \frac{1}{\Gamma(1 - \beta\cos\theta)(1+z)} \tag{31}$$

where $\mathcal{D}_{rel}$ is the relativistic doppler shift from equation 27.

Individual photon or particle energies between reference frames are related by

$$\epsilon = \frac{\epsilon_{com}}{1+z} = \mathcal{D}\frac{\epsilon^{'}}{1+z} \tag{32}$$

where ϵ, ϵ_{com} and $\epsilon^{'}$ are the energies in the observer, comoving and source frame, respectively.

The following relationships are related between source and observer frames by the Doppler factor using relativistic invariants: frequency ($\nu = \mathcal{D}\nu^{'}$), solid angle ($d\Omega = \mathcal{D}^{-2}d\Omega^{'}$), specific intensity ($I_\nu(\nu) = \mathcal{D}^3 I^{'}_{\nu^{'}}(\nu^{'})$), temperature ($T(\nu) = \mathcal{D}T^{'}(\nu^{'})$), volume ($dV = \mathcal{D}dV^{'}$), specific emissivity ($j_\nu(\nu) = \mathcal{D}^2 j^{'}_{\nu^{'}}(\nu^{'})$), specific absorption coefficient ($\mu_\nu(\nu) = \mathcal{D}^{-1}\mu^{'}_{\nu^{'}}(\nu^{'})$) and radial width ($dr = \mathcal{D}^{-1}dr^{'}$) Meszaros GRBs 2006 pg 17. The specific absorption coefficient $\mu_\nu = n\sigma_\nu$ has units of cm^{-1}, where n

is the density and σ_ν is the absorption cross-section. Both $\nu\mu_\nu$ and optical depth τ are invariants.

NEED TO CORRECT OR TAKE OUT.

A photons observed energy would be $E = E'\mathcal{D} = h\nu'\mathcal{D}$, where h is the Planck constant. The frequency of the light is related by $\nu = \nu'\mathcal{D}$ and wavelength by $\lambda = \lambda'/\mathcal{D}$, and the wavelengths of the observed light will be shortened by doppler boosting. As a result of cosmological time dilation, $E = E'(1+z)$, $\nu = \nu'(1+z)$ and $\lambda = \lambda'(1+z)$. The wavelength of light observed will be longer than when it was emitted, this is cosmological redshift. Both need to be taken into consideration, giving $E = E'(1+z)\mathcal{D}$, $\nu = \nu'(1+z)\mathcal{D}$ and $\lambda = \lambda'(1+z)/\mathcal{D}$.

1.4. **The observable cone and curvature effect.** Gamma-ray bursts have two jet-like structures, the physical jet and the observable cone; the latter as a result of relativistic beaming of the photons emitted isotropically within the jet. These photons are beamed with an opening angle proportional to the Lorentz factor of the particles within the jet, responsible for the emission. Photons emitted in the source frame perpendicular to the line of sight ($\theta' = \pi/2$) have a Doppler factor $\mathcal{D} = \Gamma^{-1}$, therefore all photons emitted in the forward direction are beamed within an observing angle $\theta_c < \Gamma^{-1}$. While the physical jet is larger than the observable jet, $\theta_j > \theta_c$, any photons emitted from a high-latitude source particle will not be observed until the observable cone grows to include it.

Using equation 27 for the limiting case ($\theta = 0$) the photons emitted along the line of sight are boosted by a factor of $\mathcal{D} \sim 2\Gamma$. Observed energies will be boosted by the same factors and require knowledge of the Lorentz factor to de-beam them. Gamma-ray bursts will appear to be more energetic and luminous to the observer than they truly are.

As discussed in the previous section, the apparent velocity of the superluminal motion is maximized at an apparent angle of Γ^{-1}, which is the edge of the observable light cone. From equations 28 and 29, we can derive the time delays between photons along the line of site and at a angle to the line of sight including cosmological effects and we get

$$
\begin{aligned}
dt &= \left(\frac{dr}{\beta c}\right)\Gamma(1-\beta\cos\theta)(1+z) \quad \text{for} \quad \frac{\pi}{2} > \theta \gg 1^\circ \\
dt &= \frac{dr(1+z)}{\Gamma\beta c} \quad \text{for} \quad \theta = \frac{1}{\Gamma} \\
dt &= \frac{dr(1+z)}{2\Gamma^2 c} \quad \text{for} \quad \theta = 0,
\end{aligned}
\tag{33}
$$

where dt is the observed times and dr are the observed locations of the photon emission and βc is the velocity of the emitting shell or particle. This is the curvature

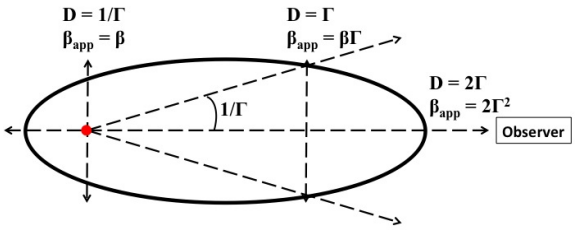

FIGURE 2. Need to update this to match mine. Plot is now mine. For a distant observer (located to the right) viewing a shell which expands spherically from S with $\Gamma = 1/\sqrt{1-(v/c)^2} \gg 1$, the locus of the points from which radiation reaches it at a later time t appears as a spheroid (equal arrival time surface). Most of the radiation arrives from the forward (right) hemisphere, which is strongly Doppler boosted inside the light cone $1/\Gamma$. The apparent transverse radius of the ellipsoid is $r_\perp \simeq \Gamma ct$, and its semi-major axis is $r_\parallel \simeq 2\Gamma ct$, where t is observer time. *Credit: Meszaros 2006*

effect; the time delay of photons emitted and the first part can be used for high-latitude emission.

As mentioned above, while $\theta_j > \theta_c$, any photons emitted from a high-latitude source particle will not be observed until the observable cone grows to include it. This is referred to as the curvature effect. The observable cone grows rapidly by a factor of $1/\Gamma$ when the fireball decelerates in addition to the continued growth as the distance from the central engine increases. During the early phase of the afterglow, the jet impacts the circumburst medium, slowing the jet, decreasing Γ and allowing for θ_c to grow. We expect a rapid, steep decay in flux since the boosting of emission is decaying as a result of the rapidly decreasing Γ. The high-latitude photons begin to enter the observable cone during this phase. At the point where the observable cone reaches the size of the physical jet, $\theta_j \simeq \theta_c \sim 1/\Gamma$, the flux decays at a much slower rate and the entire physical jet becomes observable. At the point we get the first spectral break in the canonical X-ray afterglow discussed in another section.

1.5. **Fireball Model.**

1.6. **The compactness problem.** If we assume gamma-ray bursts (GRBs) release their energy isotropically, they have been observed to emit energies exceeding $\sim 10^{54}$ ergs within seconds, which is comparable to the amount of energy released by the Sun in its lifetime CITE THIS. With a light-curve variability on the order of milliseconds, the light crossing time estimates the size of the emitting region to be a few tens or hundreds of kilometers, from the equation $R < c\Delta t/(1+z)$. Conditions within

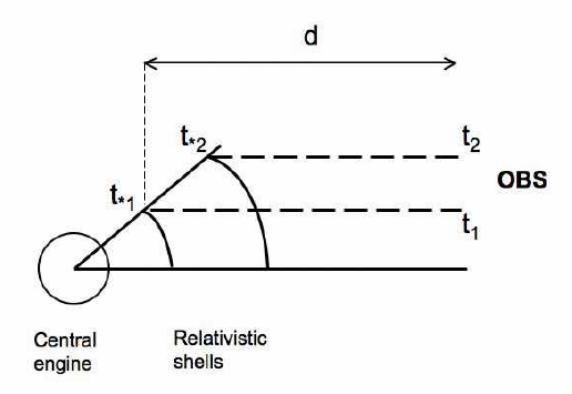

FIGURE 3. Illustration of the emission from spherical relativistic shells in the source frame and the relativistic time delay leading to the relation between source frame time and observer time. *Credit: Meszaros 2006*

such a compact fireball would allow high-energy photons to rapidly pair produce ($\gamma\gamma \rightarrow e^+e^-$) creating an extremely large optical depth ($\tau > 1$) for photons of all wavelengths. A hot dense optically thick plasma is in conflict with the non-thermal and hard spectrum revealed by many high-energy instruments. Photons above the pair production threshold ($m_e c^2$ ~1 MeV) would not survive in such an environment, but are present and abundant in several *CGRO* and *Fermi* bursts. This introduces the compactness problem.

The compactness problem originates from the assumption that the size of the emitting region can be determined by the variability in the MeV light-curve. The problem is eliminated if the source emitted the energy in another form and it was converted to the observed gamma-rays at a large distance, where the system is optically thin and $\tau_{\gamma\gamma} < 1$, (Piran 1999, $https://ned.ipac.caltech.edu/level5/March04/Piran2/frames.html$). Relativistic expansion of the emission region will reduce the rate of attenuation for photons > 1 MeV, allowing them to escape when the fireball becomes optically thin at a greater distance. Incorporating relativistic expansion, a more reasonable emission site resides at a distance of $R \sim \Gamma^2 c\Delta t/(1+z)$. For a GRB at a redshift of z =1 and Lorentz factor Γ =1000, the emission arises from a region with distance $R \sim 1$ AU from the central engine, which is a million times larger than when special relativity is ignored.

Observations of luminous CGRO EGRET and Fermi LAT bursts were found to have extremely large bulk Lorentz factors $\Gamma \geq 10^2 - 10^3$ (e.g., Lithwick & Sari 2001; Krolik & Pier 1991; Fenimore et al. 1993; Woods & Loeb 1995; Baring & Harding 1997; Abdo et al. 2009a,b,c See paper THE BULK LORENTZ FACTORS

OF FERMI-LAT GRBS). Several bright Fermi GRBs show time-integrated spectra extending up to GeV or even tens of GeV, without any signs of spectral cutoff. The emission >100 MeV also display an onset compared to the lower-energy MeV emission, revealing the higher energy emission is produced at larger radii (Li 2010)

The fireball's initial expansion happens at a highly relativistic rate, with a very high Lorentz factor ($\Gamma \gg 1$), forming a collimated jet of material emerging in opposite directions.

END HERE

Volume of the initial central engine is on the order of several Schwarzschild radii of a black hole

$$r_S = \frac{2GM_{BH}}{c^2} \quad \text{where} \quad M_{BH} \gtrsim 2M_\odot. \tag{34}$$

The final bulk Lorentz factor and the external density determine the duration of the blast wave. The dynamics of the fireball as a function of baryonic loading determines the relative amount of energy in bulk kinetic form (which gets radiated in the blast wave and reverse shock) and in pair and radiation form (which escapes when the fireball thins, usually before the blast wave burst) [**?**].

1.7. **Initial Acceleration of the Jet.** Gas temperatures of the initial GRB are so high that γ-rays readily pair produce leading to large optical depths. The plasma is opaque to photons at all energies and newly formed pairs help scatter additional photons preventing the escape of energy. As a result, the radiation pressure leads the jet to expand at a rate following the adiabatic gas law,

$$T'V'^{\gamma_a - 1} = constant, \tag{35}$$

where $\gamma_a = 4/3$ is the adiabatic index of a relativistic gas and the volume $V' \propto R^3$, so the temperature of the comoving fireball cools as it expands, $T' \propto R^{-1}$. The fireball's expansion is not purely driven by radiation pressure, rather predominantly determined by the amount of massive particles present. The amount of baryonic matter in the initial fireball determines how the jet expands; if there is too much baryonic matter the jet will be sub-relativistic. The ratio of the initial radiation to rest-mass energy of baryonic matter is given by,

$$\eta = E_0/M_0c^2, \tag{36}$$

where E_0 is the radiation energy, M_0 is the amount of baryonic matter initially contained in fireball and η is the mean energy per baryon, also referred to the baryonic load. This radiative energy $E_0 \gg M_0c^2$ is uniformly distributed throughout the jet and remains constant as the fireball evolves. This energy is considered to be the isotropic equivalent energy of the fireball.

If the initial fireball contains a very small amount of baryonic matter with low baryonic loading, the fireball will be almost purely radiative and will expand adiabatically at relativistic speeds. If the initial fireball contains a large amount of baryonic matter and large baryonic loading, the energy is trapped in the form of kinetic energy of the baryons and the jet expands at sub-relativistic speeds. There must be a good balance of radiation energy to baryonic kinetic energy in the initial fireball to allow for relativistic expansion, while still allowing for the fireball to become saturated before it becomes optically thin. At saturation, the bulk Lorentz factor has reached its maximum speed and now begins to coast.

The internal energy of the fireball is transferred into kinetic energy of the shell which can be represented by the bulk Lorentz factor

$$\Gamma = \frac{1}{\sqrt{1-\beta^2}}, \tag{37}$$

where $\beta = v/c$ represents the bulk velocity of the gas as a fraction of the speed of light as measured in the lab frame, such as the initial region of emission or the outside observer. For non-relativistic velocities, $\Gamma \sim 1$, which is the bulk Lorentz factor of the fireball within the initial radius R_{in} before expansion. The particles within R_{in} start out with a random isotropic distribution of velocities and random Lorentz factors $\gamma \sim \eta = E_0/M_0c^2$. As the fireball expands, the particles move outward and their velocity vectors are confined within an angle of $(R/R_{in})^{-1}$ along the radial direction. The expansion causes the particles to accelerate and it can be easily seen from equations 37, that the bulk Lorentz factor will increase. The initial conditions of the fireball place a maximum constraint on Γ at $\Gamma_{max} \sim \eta = E_0/M_0c^2$ at the point which all internal (thermal) energy has been converted into bulk kinetic energy carried by the matter. This is referred to as the saturation radius, R_{sat}.

Conservation of energy and thermodynamics provide a relationship between the bulk Lorentz factor and the temperature of the gas throughout this phase, $R < R_{sat}$, given by

$$E_0 = \Gamma M_0 \left(\frac{kT'}{m_p} + c^2 \right), \tag{38}$$

where the initial observed energy E_0 is a constant and the sum of the internal (thermal) plus kinetic energies. For relativistic comoving temperatures (T'), the first term dominates giving $T' \propto \Gamma^{-1}$. As the fireball expands and cools, Γ increases until $R \sim R_{sat}$ where $\Gamma \sim \Gamma_{max} = \textit{constant}$ and the matter within the shell begins to coast.

1.8. **Coasting and Spreading.** Saturation occurs at a radius determined by the initial conditions,

$$R_{sat} \sim R_{in}\eta = \frac{R_{in}E_0}{M_0c^2} \tag{39}$$

where R_{in} is the initial size of the engine. There are two main phases that occur within the fireball, radiation dominated where $R < R_{sat}$ and matter dominated where $R > R_{sat}$. During the matter dominated phase, the baryonic mass density becomes much larger than the energy density of leptons, therefore radiation processes no longer contribute to the dynamics of the jet. The matter coasts with a constant asymptotic radial velocity slightly less than c with a constant shell width.

The width of the shell appears very different to an observer than the physical size in the comoving frame. The following equations represent the width of the shell at any given radius δR, where $\delta R_{in} \sim R_{in}$ is the initial size of the engine.

$$\delta R \sim \begin{cases} \delta R_{in} & \text{for } R \leq R_\delta \\ R/\Gamma^2 & \text{for } R \geq R_\delta \end{cases} \tag{40}$$

In the observers frame of reference, equation 40, the width of the shell is the same as the size of the initial engine for most of the expansion. Even as the fireball expands at an accelerated rate during $R < R_{sat}$, Lortenz contraction makes the shell appear narrow with a constant radial width equal to R_{in}. To the observer, the fireball appears to behave like a pulse of energy with a frozen radial profile accelerating outward at almost the speed of light. This profile changes once $R \sim R_\delta$, the spreading radius, $R_\delta \sim \delta R_{in}\eta^2$, is reached and the shell begins to expand at a constant rate proportional to Γ^{-2}, which is still coasting at it's maximum.

$$\delta R' \sim \begin{cases} \delta R_{in}\Gamma \sim R & \text{for } R \leq R_{sat} \\ \delta R_{in}\eta \sim R_{sat} & \text{for } R_{sat} \leq R \leq R_\delta \\ R/\eta & \text{for } R \geq R_\delta \end{cases} \tag{41}$$

In the comoving frame of reference, equation 41, the comoving radial width, $\delta R'$, increases linearly with R since $\Gamma \propto R$ during the acceleration phase when $R < R_{sat}$. Once the saturation radius is reached, the shell's width increases by a factor of the saturation radius. The spreading radius, $R_\delta \sim \delta R_{in}\eta^2$ is a factor of η larger than the saturation radius, $R_{sat} \sim \delta R_{in}\eta$, and for large values of η spreading doesn't occur until late in the matter dominated phase.

1.9. **The Photosphere.** The initial conditions of the fireball create an extremely hot and dense plasma containing a large number of e^+e^- pairs which dominate the

scattering opacity of photons until the plasma cools and these pairs begin to recombine with the baryons. At a comoving temperature of $T' \sim 17$ keV, the recombination process begins.

The Eddington Luminosity is a limit to the maximum luminosity a source can have and remain in hydrostatic equilibrium. If the luminosity exceeds this limit, radiation pressure begins to drive outflows. This luminosity limit is

$$L_{Edd} = \eta \dot{M} c^2 = \frac{4\pi G M m_p c}{\sigma_T} = 1.26 \times 10^{38} \left(\frac{M}{M_\odot} \right) ergs^{-1}. \tag{42}$$

The extremely super-Eddington nature of these compact objects produce large optical depths to pair production (e^+e^- pairs), preventing the escape of energy in the form of photons.

The basic fireball model fails to explain observations of burst duration and temporal structure as well as the size of the emitting region. This model predicts very short burst durations that were emitted when the expanding fireball becomes optically thin.

1.10. **Internal and External Shocks.** The prompt emission occurs due to the dissipation of the jet's kinetic energy and can be explained with internal and external shocks.

In the external shock model, a single relativistic wave of particles interacts with inhomogeneities in the surrounding medium to accelerate particles that radiate the prompt gamma-rays [Dermer] through non-thermal processes. The external medium slows the fireball's relativistic outflow by transferring kinetic energy of the jet's particles to shocking the medium. The duration of the burst would be directly connected to the deceleration time and the variability of the light curves due to inhomogeneities in the interstellar medium [GRB book pg 234]. The external shock model can only predict smooth GRB light-curves instead of the fast variability observed in most. This lead [Rees and Meszaros], in 1994, to propose the internal shock model.

The internal shock model has an active central engine which ejects multiple shells with various relativistic Lorentz factors that overtake and collide to form shocks [Dermer pg 294 his citation 337]. These collisions between shells will produce a highly variable light-curve with spectral breaks that reflect the activity from the central engine. The internal shocks dissipate energy by accelerating charged particles that inturn produce high-energy synchrotron radiation.

Only a fraction of the kinetic energy is dissipated along internal shock fronts and require an external shock to follow and dissipate the remaining energy [GRB book pg 235].

accelerate non-thermal particles that radiate high-energy photons [Dermer citation 338].

The spectrum of a photosphere would be expected to look like a black-body with modifications by comptonization at higher energies cite with [343],[167],[446] from GRB paper by meszaros. We observe the spectrum as a broken power law which is highly non-thermal and suggests a mechanism for reconverting kinetic energy of the flow into random energy. Power-law spectrum we observe:

$$N(E)dE \propto E^{-\alpha}dE \tag{43}$$

where $\alpha \approx$ is the power-law index and slope of the non-thermal spectrum.

It is impossible to release such a large amount of energy in radiation without the fireball being contaminated with baryonic mass. This leads to two problems: 1) The high initial opacity would trap the bulk of the energy until it has been converted into bulk kinetic energy driving adiabatic expansion. 2) Typical time-scales for cosmological GRB models are $\sim R_0/c \sim 10^{-4}$ s based on the usual light travel time over the emitting region are far shorter than the observed time scales of ~ 10 s.

Problem 1:

If the rest mass energy of entrained baryons $> 10^5$ $M_\odot$ of the total energy, the resulting opacity would trap the radiation so that it was degraded by adiabatic expansion, and thermalized before escape. The energy would therefore be transformed into kinetic energy of the bulk relativistic outflow and the spectrum would emerge as a thermal photon spectrum instead of the non-thermal power-law we observe.

The outflow from the central engine is most likely a steady, but variable (in Lorentz factors), outflow instead of an instantaneous event.

Kinetic energy can be reconverted into gamma-rays within relativistic shocks through acceleration processes of charged particles will produce a synchrotron spectrum.

1.11. **Particle Acceleration Processes.**

1.12. **Radiation Processes.**

1.13. **Synchrotron Spectrum.** Characteristics of a synchrotron spectrum: the Lorentz factor of the relativistic electrons (γ_e), the strength of the magnetic field (B), and the Lorentz factor of the emitting material (Γ). The photons seen by the observer have been blueshifted because of the relativistic motion of the emitting material.

The energy loss-rate due to the production of synchrotron emission by accelerating charged particles in a magnetic field can be derived through the Larmor formula to get

$$-\left(\frac{dE}{dt}\right) = \frac{4}{3}\frac{8\pi}{c}\left(\frac{q_2^2}{m_e c^2}\right)^2 cU_B\beta_{par}^2\gamma_{par}^2 = \frac{4}{3}\sigma_T c U_B \beta_{par}^2\gamma^2 \tag{44}$$

where the radius of an electron $r_e = q_e^2/m_e c^2$, $U_B = B^2/8\pi$ is the magnetic energy density where B is the magnetic field strength and σ_T is the Thompson cross-section. Equation 44 is the Power emitted by synchrotron radiation and β_{par} and γ_{par} are the particle's beta factor and Lorentz factor, respectively. The subscript is typically left off of the particle Lorentz factor since γ is commonly used to represent individual particle Lorentz factors and Γ is used to represent the bulk Lorentz factor of the material in the jet.

The peak observed synchrotron frequency from a charged particle in relativistic circular motion is then

$$\nu_{peak} \approx \frac{q_e B}{2\pi m_e c}\gamma^2 \tag{45}$$

and the peak energy is

$$E_{peak} = h\nu_{peak} \approx \frac{q_e B\hbar}{m_e c}\gamma^2. \tag{46}$$

For a single electron in a single revolution at a particular frequency, these two equations become the characteristic synchrotron frequency and energy becoming

$$E_c = \frac{3}{2}\frac{q_e B\hbar}{m_e c}\gamma^2 \sin\psi \tag{47}$$

where ψ is the particle's pitch angle in an ordered magnetic field.

##

The characteristic synchrotron frequency ν_{syn} in the observer's frame is

$$\nu_{syn,obs} = \frac{q_e B}{2\pi m_e c \gamma_e^2 \Gamma} \tag{48}$$

The synchrotron power that is emitted in the comoving frame is

$$P'_{syn} = \frac{4}{3}\sigma_T c U_B \gamma_e^2 \tag{49}$$

where $U_B = B^2/8\pi = \epsilon_B e$ is the magnetic energy density and σ_T is the Thompson cross-section. The synchrotron power in the observer frame can be written as $P_{syn} = \Gamma^2 P'_{syn}$.

The synchrotron spectrum, radiated by a population of electrons with a distribution of energies, follows a power-law with an index p,

$$N(\gamma_e) \sim \gamma_e^{-p}, \tag{50}$$

where the energies (γ_e) must be greater than some minimal Lorentz factor (γ_m).

2. Jets and Collimation

Lorentz factors are expected to be $\Gamma > 10^2$ to avoid the compactness problem.

In order to overcome the compactness problem for GRBs, the jets are believed to be highly collimated into a bio-polar with a half-opening angle of θ_j, representing its physical size. *The compactness problem will be discussed in a later section.*

The photons received from a highly relativistic jet are beamed in the observer's frame of reference and the level of beaming is dependent on the relativistic bulk motion of the emitting plasma, represented by the bulk Lorentz factor (Γ). A source emitting photons isotropically, in its frame, will be beamed into a cone with a half-opening angle $\theta_b \sim \frac{1}{\Gamma}$, as seen in the observer's frame of reference. This angle should not to be confused with the half-opening angle of the GRB's physical jet, θ_j.

Initially, the physical jet is wider than the observable cone ($\theta_b < \theta_j$) and photons emitted at high-latitudes to the line-of-sight can not be observed. This is known as the curvature effect. At this point, only a fraction of the jet can be observed and it can not be distinguished if the GRB is emitting isotropically as seen in the spherical case, or anisotropically as seen in the collimated jet case, *see Figure 4.*

The observable jet angle, θ_b, widens as the distance from the apex of the cone, R, increases. Once the jet hits the circum-burst medium it begins to decelerate, Γ decreases and θ_b widens quickly at a rate determined by R/Γ. Prior to this, the jet is in the coasting phase and Γ is constant. When the observable area grows to match the size of the jet ($\theta_b \sim \theta_j$), the entire jet becomes visible and an achomatic break is expected in the light-curve and observed as t_{b1} in the canonical afterglow. For the spherical case, this break does not occur.

Some of the high-latitude photons emitted at angle θ during the prompt phase will be delayed by $t = (1+z)(R/c)(\theta^2/2)$ and received as θ_b grows during Phase I of the afterglow. The curvature effect introduces a relationship between the temporal index, α, and the spectral index, β, implying the flux will decay with the temporal slope by $\alpha = 2+\beta$ *Zhang et al. 2006, Kumar & Panaitescu 2000, Dermer 2004, and Panaitescu et al. 2006b - GRB book pg 334.* This sharp flux decay has been found to be in rough agreement with many observations *Panaitescu 2006, O'Brien et al. 2006, and Nousek et al. 2006 - GRB book pg 334*

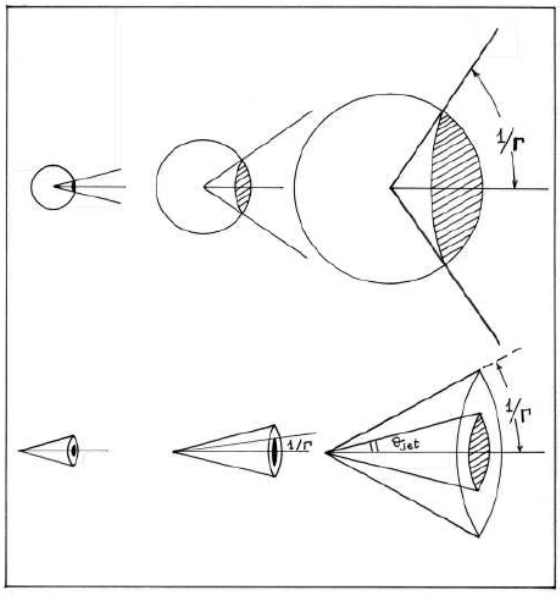

FIGURE 4. From Ghisellini 2001 (general GRB's folder), this figure shows two possible explanations for the transition between the prompt and afterglow phases. In the initial stage of the afterglow, the bulk Lorentz factor is large and the observer only sees a fraction of the emitting area within the cone of aperture angle $\sim 1/\Gamma$. At this stage, the spherical and collimated jet cases are exactly the same. In the spherical case, the emitting area grows as a factor of the increase in radius and because Γ decreases, allowing more surface to be within the $1/\Gamma$ cone. In the collimated jet case, the observed surface increases only because the distance to the jet apex increases to the point where the In the case of collimation in a jet, once $1/\Gamma$ becomes comparable to the jet opening angle θ, the observed surface increases only because the distance to the jet apex increases. The light curve predicted in the two cases is therefore the same at early times, but in the jet case there will be a break at a particular time (when $1/\Gamma \sim \theta$), after which the light curve decreases more rapidly than in the spherical case.